



# Numerical simulation of heat and fluid flow in basic pulse tube refrigerator

Numerical simulation

617

Takao Koshimizu

*Department of Mechanical Engineering, Kitakyushu National College of Technology, Kitakyushu, Japan*

Hiromi Kubota and Yasuyuki Takata

*Department of Mechanical Engineering Science, Kyushu University, Fukuoka, Japan, and*

Takehiro Ito

*Graduate School of Integrated Science and Art, University of East Asia, Shimonoseki, Japan*

Received May 2003  
Revised December 2003  
Accepted October 2004

## Abstract

**Purpose** – To clarify the physical working principle of refrigeration in basic pulse tube refrigerators (BPTRs).

**Design/methodology/approach** – A numerical simulation was performed. Transient compressible NS equation was solved utilizing the TVD scheme coupled with energy equation.

**Findings** – The periodic flow and temperature field were obtained. The movement of the gas particles and heat transfer between the gas particles and wall were analyzed. These numerical results explained the mechanism of surface heat pumping (SHP) which is known as the working principle of refrigeration in BPTR.

**Research limitations/implications** – Pulse tube refrigerator (PTR) is classified into the third generation. BPTR is the first generation. It is needed to clarify the working principle of refrigeration in the second and third generation by analyzing heat and fluid flow in the tube.

**Practical implications** – A very useful source of information to understand the physical working principle of refrigeration in BPTR.

**Originality/value** – The mechanism of SHP was shown by analyzing the heat exchange between the gas particles and pulse tube wall.

**Keywords** Heat transfer, Refrigeration, Pulsating flow

**Paper type** Research paper

## Nomenclature

$a$	= thermal diffusivity of wall ( $\text{m}^2/\text{s}$ )	$f$	= friction force vector ( $\text{N}/\text{kg}$ )
$A$	= heat transfer area ( $\text{m}^2$ )	$L_p$	= length of pulse tube ( $\text{m}$ , $\text{mm}$ )
$A'$	= heat transfer area per unit volume ( $\text{m}^2/\text{m}^3$ )	$M$	= mass of regenerator material ( $\text{kg}$ )
$c$	= specific heat ( $\text{J}/(\text{kg K})$ )	$p$	= pressure ( $\text{Pa}$ )
$e$	= total of internal energy and kinetic energy ( $\text{J}/\text{kg}$ )	$Q$	= heat transfer rate per unit volume ( $\text{W}/\text{m}^3$ )
$f$	= friction force ( $\text{N}/\text{kg}$ )	$r$	= radial coordinate ( $\text{m}$ , $\text{mm}$ )
		$r_{\text{in}}$	= radius to the inner wall in pulse tube ( $\text{m}$ , $\text{mm}$ )



$r_{out}$ = radius to the outer wall in pulse tube (m, mm)	$\Phi$ = energy dissipation function ( $W/m^3$ )
$R$ = gas constant ( $J/(kg K)$ )	$\lambda$ = thermal conductivity ( $W/(m K)$ )
$t$ = time (s)	$\mu$ = coefficient of viscosity ( $Pa s$ )
$T$ = temperature (K)	$\rho$ = density of working gas ( $kg/m^3$ )
$V$ = velocity (m/s)	$\tau$ = shearing stress (Pa)
$\mathbf{V}$ = velocity vector (m/s)	
$x$ = axial coordinate (m, mm)	<i>Subscripts</i>
$x_p$ = length from the boundary between regenerator and pulse tube (m, mm)	gas = working gas
$x_{rg}$ = length from the open end in regenerator (m, mm)	in = inlet of regenerator
$\alpha$ = heat transfer coefficient ( $W/(m^2 K)$ )	$r$ = radial direction in pulse tube
$\varepsilon$ = internal energy (J/kg)	rm = regenerator material
	w = wall (stainless steel layer)
	$x$ = axial direction
	$xr$ = surface of $x-r$

### Introduction

Pulse tube refrigerator (PTR) has a very originitive characteristic that there is no moving parts at low temperatures, which leads to mechanical simplicity, high reliability, low vibration and long life. Therefore, PTR is expected to be used for cooling of superconducting devices and in the field of medicine and space.

PTR was invented in 1963 by Gifford and Longsworth (1964), which is now called basic pulse tube refrigerator (BPTR) classified into the first generation. In 1984, orifice pulse tube refrigerator (OPTR) classified into the second generation was invented by Mikulin *et al.* (1984). In 1990, double inlet pulse tube refrigerator (DPTR) classified into the third generation was invented by Zhu *et al.* (1990). Researches and developments for optimal design and efficient operation of PTR have been done up to now. Now the lowest temperature and COP of PTR became equivalent to those of the G-M and the stirling refrigerators. Researches on the working principle of refrigeration such as a visualization of the heat and fluid flow in the pulse tube (Shiraishi *et al.*, 1998) and numerical simulation (Hozumi *et al.*, 1998) have also been performed, however, the working principles for PTRs of three generations do not seem to be made clear except for those explained by thermoacoustic theory (Tominaga, 1989). The thermoacoustic theory was successful in explaining the working principle by introducing a new concept for the oscillatory flow such as heat flow, work flow and enthalpy flow. However, when we would like to understand the physical working principle of refrigeration in PTR by explaining the transient behavior of heat and fluid flow in the pulse tube during a cycle, we cannot use the thermoacoustic theory because it is analyzed by using the temporal average quantities such as heat flow, work flow and enthalpy flow in thermoacoustic theory.

Gifford and Longsworth (1965) Gifford proposed a qualitative explanation called surface heat pumping (SHP) as a working principle of refrigeration. The refrigeration effect occurs by the mechanism of SHP that the heat is conveyed from the cold end to hot end of the pulse tube by the successive heat exchange between the working gas and pulse tube wall. Though Hozumi *et al.* performed a numerical simulation in which the transient axisymmetric two-dimensional equations were directly solved, they considered the pulse tube wall to be adiabatic wall and neglected the heat exchange between the working gas and pulse tube wall. However, considering the heat exchange between the working gas and pulse tube wall is essential to explain the mechanism of SHP.

A numerical simulation has been performed to analyze the SHP. Transient compressible NS equation coupled with energy equation was solved utilizing the TVD scheme. As a result, the behavior of gas temperatures in the pulse tube and in the regenerator, and wall temperature were shown first. Next, the mechanism of SHP was shown by analyzing the heat exchange between the gas particles and pulse tube wall.

**Physical model**

Physical model for numerical simulation is shown in Figure 1. The pulse tube is a stainless steel pipe of 150 mm in length, 5 mm in inner diameter and 1 mm in thickness. The outer wall of 30 mm in length from the closed end of pulse tube is kept at constant temperature of 290 K to be represented as heat exchanger. Heat load of 10 mW is given at the outer wall between  $x_p = 0$  and 30 mm in the pulse tube, however, it is calculated under the condition of no heat load until a cyclic steady state is attained. After a cyclic steady state under the condition of no heat load is attained, the heat load is given and a cyclic steady state is achieved again. It is considered to be adiabatic at the outer wall of the pulse tube except for the part in which the heat load is given ( $x_p = 0 \sim 30$  mm) and the part of the heat exchanger ( $x_p = 120 \sim 150$  mm). However, the heat exchange between the working gas and inner wall of the pulse tube is assumed to be convective heat transfer. The dimensions of the regenerator are 60 mm in length and 12.5 mm in inner diameter. It is assumed that woven 200 mesh wire screens of copper are filled as the regenerator material. The gas temperature at the open end of the regenerator ( $x_{rg} = 0$  mm) is kept at constant temperature of 290 K. Air is selected as the working gas. The oscillating flow is generated by changing the pressure at the open end of the regenerator as a sinusoidal wave.

It is selected as the initial condition that the pressure is 0.1 MPa and temperatures of the working gas, stainless steel pipe and regenerator material are 290 K. It is chosen as the operating condition that the pressure ratio is 2 and operating frequency is 1 Hz.

Although the initial pressure and pressure ratio are lower compared with those in actual PTR, the present condition is sufficient enough to explain the mechanism of SHP.

The expression of “initial cycles” and “a cyclic steady state” are used in numerical results. Initial cycles means the period within around 10 s from the beginning of calculation. A cyclic steady state means the state that the changes in the pressure,

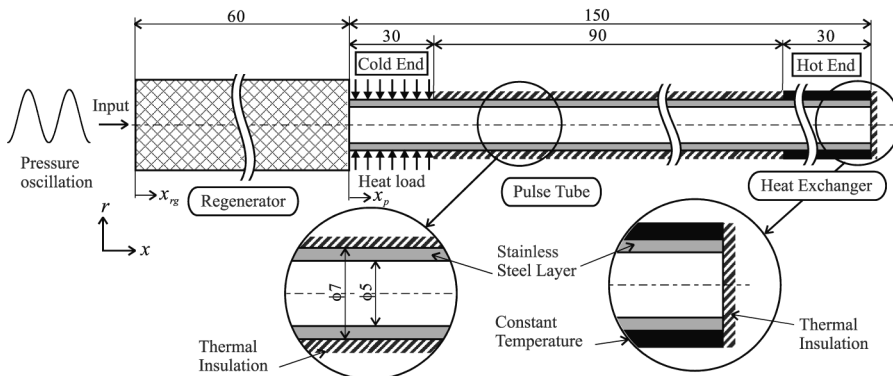


**Figure 1.**  
Physical model

temperature, velocity and density, etc. during a cycle are periodically the same. It is calculated under the condition of no heat load in initial cycles, and heat load of 10 mW in a cyclic steady state.

### Governing equations

The basic assumptions are as follows:

- (1) Heat transfer and fluid flow in the pulse tube are axisymmetric two-dimensional, while those in the regenerator are one-dimensional. The regenerator is considered as the porous materials.
- (2) The flow in the pulse tube is viscous compressible and that in the regenerator compressible.
- (3) The working gas is an ideal gas.
- (4) Thermal conductivities, heat capacities and kinetic viscosity are assumed to be independent of temperature.
- (5) The term of gravity in energy equation is neglected.

Under these assumptions, the basic governing equations are written as follows.

Continuity equation for gas

$$\frac{\partial \rho}{\partial t} + (\mathbf{V} \cdot \nabla) \rho = -\rho(\nabla \cdot \mathbf{V}) \quad (1)$$

Momentum equation for gas

$$\rho \frac{\partial \mathbf{V}}{\partial t} + \rho(\mathbf{V} \cdot \nabla) \mathbf{V} = -\nabla p + \rho \mathbf{f} \quad (2)$$

where in case of gas calculation in the regenerator,  $\mathbf{f}$  is neglected. On the other hand, in case of gas calculation in the pulse tube,  $\mathbf{f}$  is given by the following:

$$\mathbf{f} = (f_x, f_r) \quad (3)$$

$$f_x = \frac{1}{\rho} \left[ \frac{\partial \tau_{xx}}{\partial x} + \frac{1}{r} \frac{\partial (r \tau_{xr})}{\partial r} \right] \quad (4)$$

$$f_r = \frac{1}{\rho} \left[ \frac{\partial \tau_{xr}}{\partial x} - \frac{\tau_{\theta\theta}}{r} + \frac{1}{r} \frac{\partial (r \tau_{rr})}{\partial r} \right] \quad (5)$$

where

$$\tau_{xx} = 2\mu \frac{\partial V_x}{\partial x} - \frac{2}{3} \mu \operatorname{div} \mathbf{V} \quad (6)$$

$$\tau_{\theta\theta} = 2\mu \frac{V_r}{r} - \frac{2}{3} \mu \operatorname{div} \mathbf{V} \quad (7)$$

$$\tau_{rr} = 2\mu \frac{\partial V_r}{\partial r} - \frac{2}{3} \mu \operatorname{div} \mathbf{V} \quad (8)$$

Energy equation for gas

Numerical  
simulation

$$\rho \frac{\partial e}{\partial t} + \rho(\mathbf{V} \cdot \nabla)e = -\mathbf{V} \cdot \nabla p + \rho(\mathbf{V} \cdot \mathbf{f}) - p(\nabla \cdot \mathbf{V}) + \Phi + Q \quad (9)$$

where

$$e = \varepsilon + \frac{1}{2}(V_x^2 + V_r^2) \quad (10)$$

$$\Phi = \tau_{xx} \left( \frac{\partial V_x}{\partial x} \right) + \tau_{rr} \left( \frac{\partial V_r}{\partial r} \right) + \tau_{\theta\theta} \left( \frac{V_r}{r} \right) + \tau_{xr} \left( \frac{\partial V_x}{\partial r} + \frac{\partial V_r}{\partial x} \right) \quad (11)$$

$$Q = \lambda_{\text{gas}} \nabla^2 T_{\text{gas}} + \alpha A' (T_{\text{rm}} - T_{\text{gas}}) \quad (12)$$

In case of gas calculation in the regenerator,  $\mathbf{f}$  and  $\Phi$  are neglected. In equation (12), the first term of the right-hand side represents thermal conduction, which appears both in the regenerator and pulse tube. The second term means the heat exchange between the working gas and regenerator material, which appears only in the regenerator calculation.  $A'$  in equation (12) is a heat transfer area per unit volume, which is estimated from actual refrigerator in author's experimental apparatus.

The preceding equations (1), (2), (9) and the following equation (13) were used for gas calculation in the regenerator and pulse tube.

$$p = \rho RT \quad (13)$$

It was decided as the boundary condition of the open end of the regenerator ( $x_{\text{rg}} = 0$  mm) that the pressure was changed as sinusoidal wave and the gas temperature flowing into the regenerator was constant. The wall boundary that the velocity was 0 was used at the inner wall of the pulse tube ( $r = r_{\text{in}}$ ) and the closed end of the pulse tube ( $x = L_p$ ). The symmetric boundary was applied at the center in axial direction of the pulse tube. The regenerator and pulse tube were connected so that the conservation laws might be satisfied. The gas and wall were connected by considering convective heat transfer.

In above-mentioned four equations for gas, a first-order up-wind TVD scheme (Yee, 1987) was applied to the others except for the convection term and a second-order central difference was applied to the others for the convection term in space. The time integration was performed explicitly (first-order temporal accuracy). All grids used for gas calculation in the pulse tube and in the regenerator were constructed in the  $x \times r$  and  $x$  computational domain, respectively. The uniform grids were selected in this calculation. In the pulse tube, the numbers of grids in  $x$  and  $r$  directions were 50 and 10, respectively. In the regenerator, the number of grid in  $x$  direction was 20.

Energy equation for regenerator material

$$c_{\text{rm}} M \frac{\partial T_{\text{rm}}}{\partial t} + \alpha A (T_{\text{gas}} - T_{\text{rm}}) = 0 \quad (14)$$

It was assumed that the regenerator material exchanged the heat only with gas, however, the heat transfer in axial direction between regenerator materials was ignored.

Equation (14) was solved by an explicit scheme (first-order temporal accuracy) with respect to time. The uniform grids were selected in this calculation and the number of grids in  $x$  direction was 20.

Thermal conduction equation for pulse tube wall

$$\frac{\partial T_w}{\partial t} = a \nabla^2 T_w \tag{15}$$

It was decided as the boundary condition that it was adiabatic at the outer wall of the pulse tube ( $r = r_{out}$ ) except for the part of heat exchanger ( $x_p = 120 \sim 150$  mm).

The equation (15) was solved by a second-order central difference in space and SOR method in time. All grids used for wall calculation were constructed in the  $x \times r$  computational domain. The uniform grids were selected in this calculation and the numbers of grids in  $x$  and  $r$  directions were 50 and 4, respectively.

We made a Fortran program for this analysis and the calculation was continued by a personal computer until achieving a cyclic steady state.

**Numerical results**

*Analysis in initial cycles*

Figure 2 shows the behavior of pressures in the regenerator and pulse tube during the initial five cycles. The pressures shown in Figure 2 are at the cold ends ( $x_p = 5$  mm,  $r = 0$  mm in the pulse tube,  $x_{rg} = 55$  mm in the regenerator), center points ( $x_p = 75$  mm,  $r = 0$  mm in the pulse tube,  $x_{rg} = 30$  mm in the regenerator) and hot ends ( $x_p = 145$  mm,  $r = 0$  mm in the pulse tube,  $x_{rg} = 5$  mm in the regenerator) of the regenerator and pulse tube. However, it can be seen that only one pressure wave is shown in Figure 2 because all the pressure waves at above-mentioned six points overlap each other. It can be confirmed that the sinusoidal pressure waves are generated in the regenerator and pulse tube by the pressure wave given as a boundary condition at the open end of the regenerator.

Figure 3 shows the behavior of gas temperatures at the cold end of the pulse tube ( $x_p = 5$  mm,  $r = 0$  mm), hot end of the pulse tube ( $x_p = 145$  mm,  $r = 0$  mm) and cold end of the regenerator ( $x_{rg} = 55$  mm) during the initial ten cycles. It can be seen that the lowest gas temperatures at the cold end and hot end of the pulse tube during expansion are almost the same as each other, however, the gas temperature at the cold end of the pulse tube does not increase so much as that at the hot end of the pulse tube

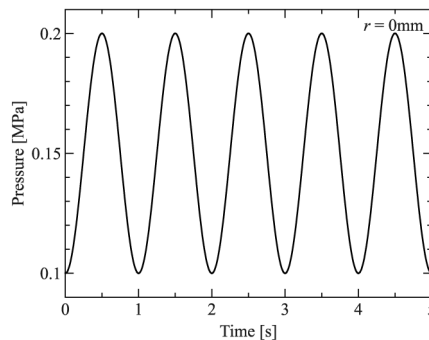
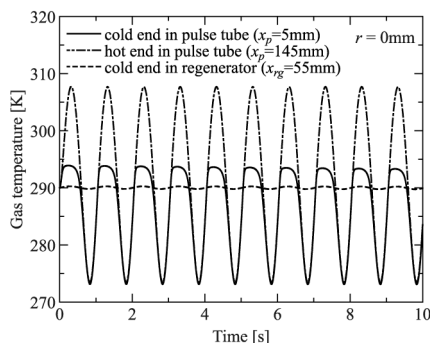


**Figure 2.**  
Behavior of pressures in the regenerator and pulse tube during the initial five cycles

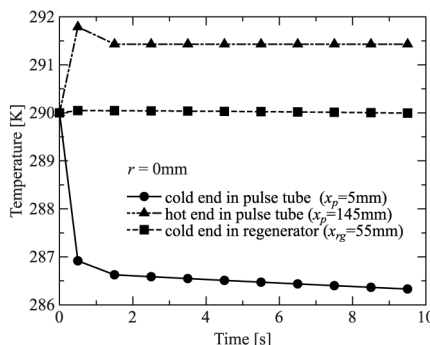
during compression. It is considered that the small increase in gas temperature at the cold end during compression is due to the gas flowing into the pulse tube after passing through the regenerator in which the change in gas temperature is limited because the gas transfers its heat to the regenerator material. It is found that the change in gas temperature in the regenerator is very small compared with that in the pulse tube. This is due to the sufficient heat exchange between the gas and regenerator material.

Figure 4 shows the behavior of the changes in gas temperatures that are the cycle average of each temperature waves corresponding to Figure 3. The gas temperature at the cold end of the pulse tube decreases rapidly in the first one cycle and then gradually decreases with time. It is conceived that the initial rapid decrease is due to the limit of increase in gas temperature by the wall during compression and the gradual decrease after the rapid decrease is due to the small decrease in temperature of the wall and regenerator material which have large heat capacity. On the other hand, the gas temperature at the hot end of the pulse tube becomes constant after the initial rapid increase because of the effect of the heat exchanger whose circumference is kept at constant temperature of 290 K. It is also confirmed that the change in gas temperature in the regenerator is considerably small compared with that in the pulse tube. Therefore, only the change in gas temperature in the regenerator is shown in Figure 5.

Figure 5 shows the behavior of temporal average gas temperatures at the hot end ( $x_{rg} = 5\text{ mm}$ ), center point ( $x_{rg} = 30\text{ mm}$ ) and cold end ( $x_{rg} = 55\text{ mm}$ ) in the regenerator during the initial ten cycles. The gas temperature at the center point



**Figure 3.**  
Behavior of gas temperatures in the regenerator and pulse tube during the initial ten cycles



**Figure 4.**  
Behavior of temporal average gas temperatures in the regenerator and pulse tube during the initial ten cycles

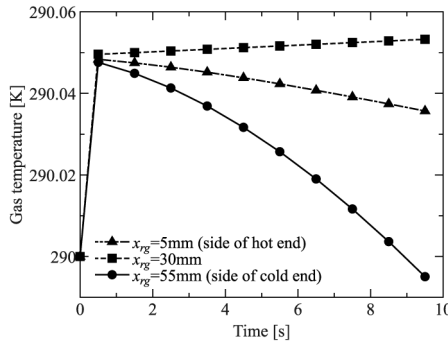
increases gradually and reversely those at the hot end and cold end decrease with time. The decrease in gas temperature at the cold end is especially remarkable, and the temperature becomes lower than 290 K of the initial temperature in about 9 s. This is due to the decrease in gas temperature at the cold end of the pulse tube as shown in Figure 4. Though the change in temperature of the regenerator material is not shown here, it has already been confirmed that the change in temperature of the regenerator material is similar to the change in gas temperature in the regenerator.

Figure 6 shows the behavior of wall temperatures at the cold end ( $x_p = 5$  mm), center point ( $x_p = 75$  mm) and hot end ( $x_p = 145$  mm) during the initial ten cycles. All the temperatures in Figure 6 are at the depth of 0.125 mm from the inner wall of the pulse tube. The wall temperature at the cold end decreases with time and become lower than 290 K of initial temperature during the first one cycle. This is due to the effect of the decrease in gas temperature at the cold end of the pulse tube. Also the wall temperature at the hot end hardly changes because of the effect of the heat exchanger.

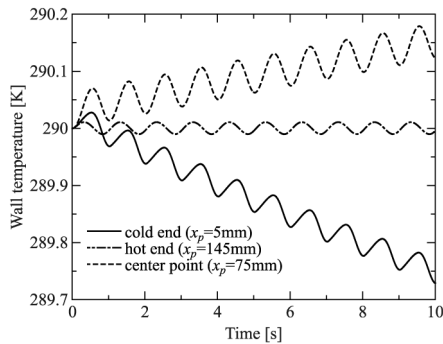
*Analysis in a cyclic steady state*

Figure 7 shows the behavior of gas and wall temperatures at the points of  $x_p = 5, 20, 45, 75$  and 145 mm in a cyclic steady state. All the gas temperatures are at the center point in radial direction. All the wall temperatures are at the depth of 0.125 mm from the inner wall of the pulse tube. The changes in gas temperatures at the points that are closer to the regenerator are limited by the gas entering the pulse tube after passing

**Figure 5.**  
Behavior of temporal average gas temperatures in the regenerator during the initial ten cycles

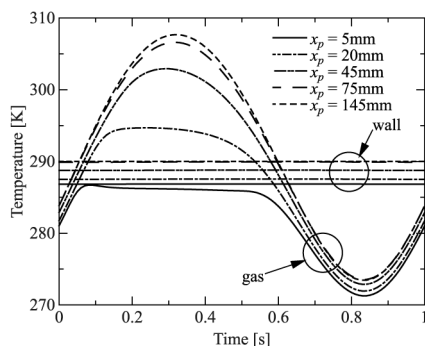


**Figure 6.**  
Behavior of wall temperatures during the initial ten cycles





**Figure 7.** Behavior of gas and wall temperatures in a cyclic steady state



through the regenerator during compression. There is no qualitative difference between the behaviors of gas temperatures in initial cycles and in a cyclic steady state, however, it is confirmed that the gas temperatures at all points shown in Figure 7 are lower than the wall temperatures in each point at the time of the beginning of compression in a cyclic steady state. It is also confirmed that the gas temperature at the point of  $x_p = 5$  mm is not higher than the wall temperature during a cycle. Therefore, it is expected that the heat is always transferred from the wall to the working gas at the point of  $x_p = 5$  mm during a cycle.

Figures 8 and 9 show the axial temporal average temperature profiles of the gas in the pulse tube and wall, and the total amount of the heat exchange between the working gas and wall during a cycle in a cyclic steady state, respectively. In Figure 8, the gas temperatures at all three points are at the points of  $r = 0, 1$  and  $2$  mm, and the wall temperature is at the depth of  $0.125$  mm from the inner wall of the pulse tube. In Figure 9, the negative value means the heat transfer from the wall to the working gas, and reversely the positive value means the heat transfer from the working gas to the wall. The gas temperature is lower than the wall temperature at the left side of the point of  $x_p = 35$  mm and the heat is transferred from the wall to the working gas as shown in Figures 8 and 9. The heat transfer from the wall to the working gas near the open end of the pulse tube is remarkably large compared with those at other points. Also the gas temperature is higher than the wall temperature at the right side of the point of  $x_p = 35$  mm, and there, the heat is transferred from the working gas to the wall. As a result, it is found that the heat is removed from the wall at the cold end

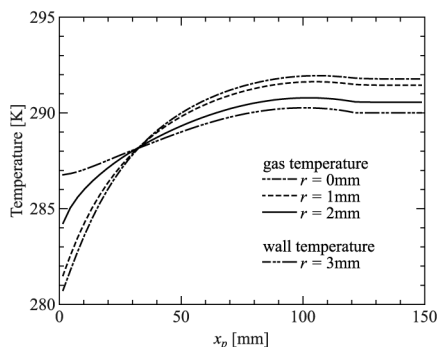


**Figure 8.** Temporal average temperature profiles of the gas in the pulse tube and the wall during a cycle in a cyclic steady state

because the gas temperature is lower than the wall temperature, which is very important for PTR to be used actually as a refrigerator.

*Analysis about surface heat pumping*

Figure 10 shows the effect of SHP performed by a gas particle in the first one cycle from the beginning of calculation. A gas particle located at the point of  $x_p = 5$  mm

**Figure 9.**  
Heat transfer from the working gas to the wall during a cycle in a cyclic steady state

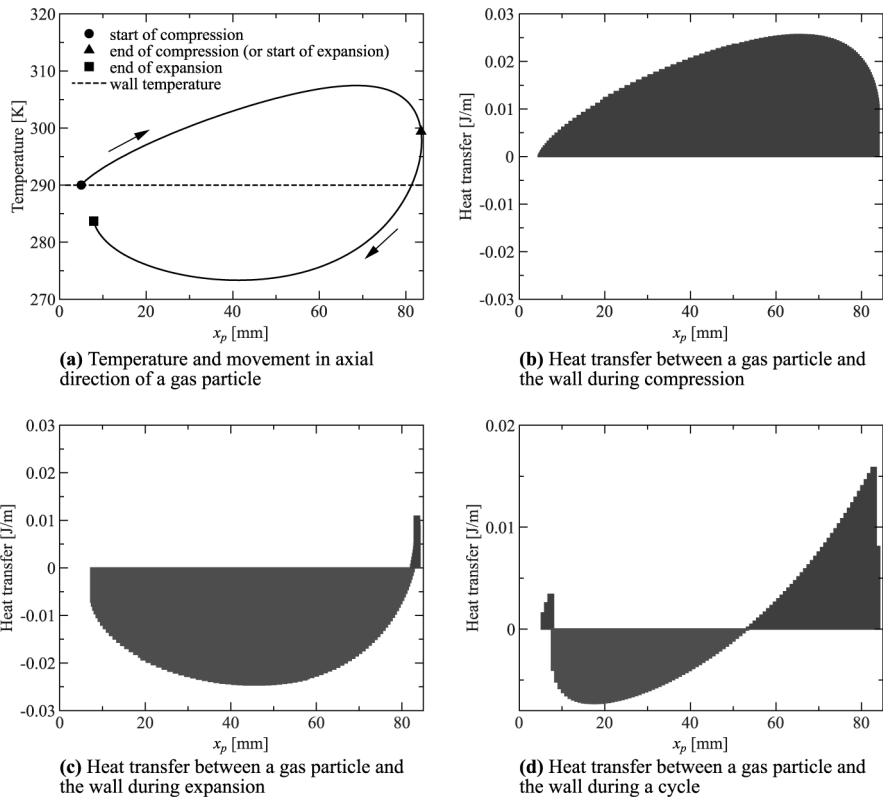
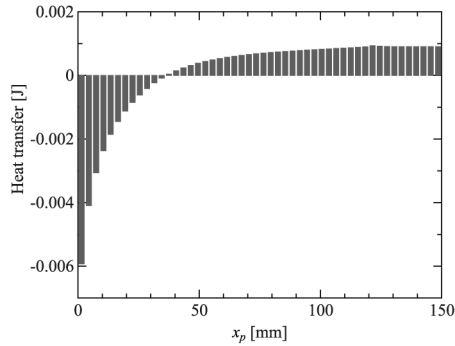


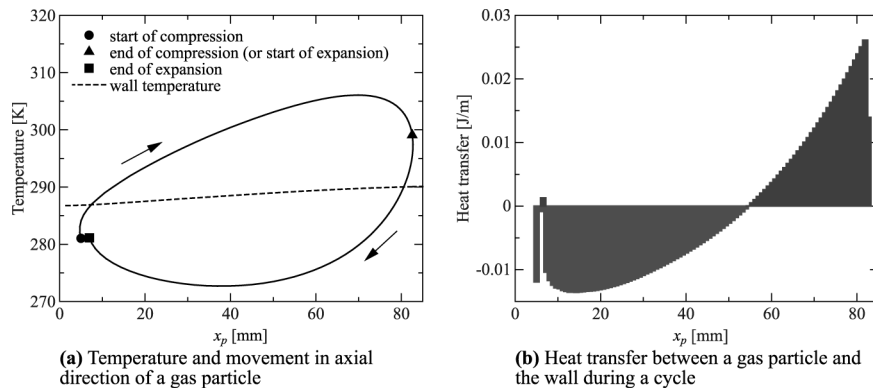
**Figure 10.**  
SHP for a gas particle in the first one cycle

and  $r = 0$  mm at the time of the beginning of compression was selected as a target. Figure 10(a) shows the movement in axial direction and the change in temperature of the gas particle. The gas particle shown in Figure 10(a) moves toward to the side of the hot end as increasing its temperature and then begins to decrease its own temperature before reaching the point of the end of compression. In the matter of this decrease in temperature of the gas particle, it is conceived that the effect of the temperature decrease by the heat exchange between the gas particle and wall is stronger than that of the temperature increase by the pressurization of the gas in the pulse tube. Reversely, the gas particle moves toward to the side of the cold end as decreasing its temperature up to the point of about  $x_p = 40$  mm during expansion and then moves as increasing temperature from that point to the point of the end of expansion. It is considered that the effect of the temperature increase by the heat exchange between the gas particle and wall is stronger than that of the temperature decrease by depressurization of the gas in the pulse tube. Figure 10(b) and (c) shows the total amount of the heat exchange per unit length between the gas particle and wall during compression and expansion, respectively. Actually the heat is not directly exchanged between the gas particle and wall because there are many other gas particles between the gas particle and wall. However, in this analysis it is defined that the heat is rapidly exchanged between the gas and wall, and the heat transfer between the gas particle and wall is considered as that between the gas and wall at the axial position in which the gas particle is located. In Figure 10(b) and (c), the negative value means the heat transfer from the wall to the gas particle, and the positive value means the heat transfer from the gas particle to the wall. In Figure 10(b), the heat is transferred from the gas particle to the wall at any time during compression and the point at maximum temperature is located in the side of the hot end. Therefore, it is found that the heat is transferred mainly from the gas particle to the wall in the side of the hot end rather than in the side of the cold end. In Figure 10(c), the gas particle moves toward to the cold end as receiving the heat from the wall. Total amount of the heat exchange per unit length between the gas particle and wall during a cycle, that is the superposition of Figure 10(b) and (c) is shown in Figure 10(d). Figure 10(d) shows that the gas particle receives the heat from the wall in the side of the cold end and gives the heat to the wall in the side of the hot end during a cycle. It is supposed that this is exactly SHP that the heat is pumped from the side of the cold end to the side of the hot end by the successive heat exchange between the gas particle and the wall. It can be seen that the heat is transferred from the gas particle to the wall in the part between  $x_p = 5$  and 7.9 mm in Figure 10(d) because the influence of heat exchange only during compression is shown in this part. In the compression process, the gas particle moves from the position of  $x_p = 5 - 83.5$  mm. On the other hand, in the expansion process, the gas particle moves from the position of  $x_p = 83.5 - 7.9$  mm (does not return to the position of  $x_p = 5$  mm). Therefore, in the part between  $x_p = 5$  and 7.9 mm, the behavior of heat exchange only during compression is shown in Figure 10(d). That the gas particle does not return to the position at the time of the beginning of compression is due to the total heat amount exchanged between the gas and wall during a cycle. It is understandable by considering the change in volume of the space between a gas particle in the pulse tube and the closed end of the pulse tube. If there is no heat exchange between the gas in this volume and the wall, the gas particle returns to the initial position because the changes in this volume during compression and expansion are equal. However, if there is

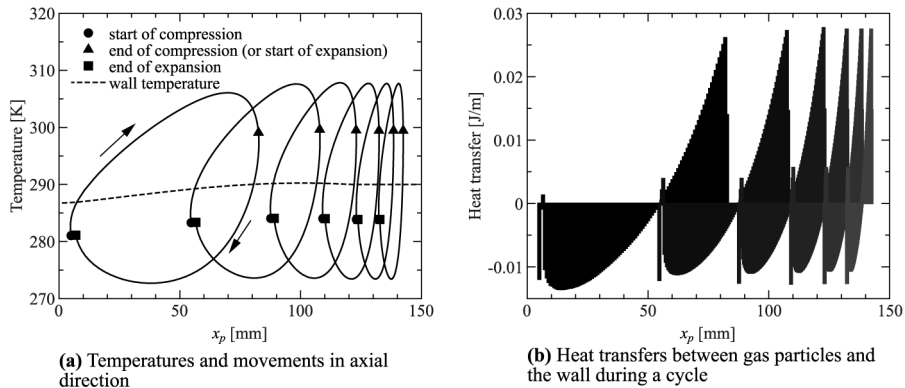
the heat exchange, these changes in this volume are different because there is the inflow or outflow of heat to this volume. The change in volume during compression is larger than that during expansion because the heat removed from the gas during compression is larger than the heat received from the wall during expansion. This is the reason why the gas particle does not return to the initial position in initial cycles.

Figure 11 shows the behavior of SHP performed by a gas particle in a cyclic steady state. Figure 11(a) shows the movement in axial direction and the change in temperature of the gas particle. The gas particle selected as a target is the same as the particle shown in Figure 10(a). There is no qualitative difference between the result analyzed in a cyclic steady state and that in the first one cycle. The gas particle does not return to the initial position in spite of a cyclic steady state. It is considered that this is due to numerical error and possibly the generation of a secondary flow, however, it is not a big problem to explain the SHP. Figure 11(b) shows the total amount of the heat exchange per unit length between the gas particle and wall during a cycle in a cyclic steady state. There is no qualitative difference between the result analyzed in a cyclic steady state and that in the first one cycle shown in Figure 10(d), however, there is a quantitative difference that the heat pumped from the side of the cold end to the side of the hot end in a cyclic steady state increases compared with that in the first one cycle because the heat load is given at the cold end in a cyclic steady state.

It is confirmed that the heat is pumped from the side of the cold end to the side of the hot end along the movement of a gas particle, however, it is necessary that the heat is pumped from the cold end to the hot end because the heat is finally removed at heat exchanger located in the hot end in the pulse tube. Therefore, the mechanism of SHP performed by several gas particles is shown in Figure 12. Figure 12(a) shows the movements in axial direction and the changes in temperatures of several gas particles, and Figure 12(b) the movements in axial direction and the total amount of the heat exchange per unit length between the gas particles and wall during a cycle in a cyclic steady state. A gas particle receives the heat transferred from another gas particle through the intermediary of the wall and then gives that heat to the wall at the point further toward the hot end as shown in Figure 12. The moving distances of gas particles in the side of the hot end are shorter than those in the side of the cold end, however, finally heat is pumped to the hot end. It can be understood that this heat pumping is SHP.



**Figure 11.**  
SHP for a gas particle in a cyclic steady state



**Figure 12.** SHP for several gas particles in a cyclic steady state

### Conclusion

A numerical simulation of viscous compressive flow in BPTR was performed to analyze the heat and fluid flow in pulse tube and make clear the behavior of SHP. The results are as follows:

- (1) Initial rapid decrease in temporal average gas temperature at the cold end of the pulse tube is due to the limit of the increase in gas temperature during compression, and gradual decrease after that is due to the effect of the decrease in gas temperature at the cold end of regenerator and pulse tube wall.
- (2) The behaviors that the gas particle receives the heat from the wall at the cold end of the pulse tube and that the gas particle transfers the heat to the wall at the hot end of the pulse tube were confirmed by analyzing the heat exchange between the gas particle and the wall.
- (3) The effect of storing heat in the wall is confirmed by visualizing the mechanism of SHP, that is heat pumping from the cold end to the hot end of the pulse tube, which leads to importance of the wall.

### References

- Gifford, W.E. and Longworth, R.C. (1964), "Pulse-tube refrigeration", *Journal of Engineering for Industry*, Trans. ASME, Series B, Vol. 86, pp. 264-8.
- Gifford, W.E. and Longworth, R.C. (1965), "Surface heat pumping", *Advances in Cryogenic Engineering*, Vol. 11, pp. 171-9.
- Hozumi, Y., Murakami, M. and Yoshizawa, Y. (1998), "Numerical study of pulse-tube flow", *Cryogenic Engineering*, Vol. 33 No. 4, pp. 200-6 (in Japanese).
- Mikulin, E.I., Tarasov, A.A. and Shkrebyonock, M.P. (1984), "Low-temperature expansion pulse tube", *Advances in Cryogenic Engineering*, Vol. 29, pp. 629-37.
- Shiraishi, M., Nakamura, N., Murakami, M. and Nakano, A. (1998), "Visualization study of flow behavior in pulse tube refrigerator", *Cryogenic Engineering*, Vol. 33 No. 4, pp. 249-57 (in Japanese).
- Tominaga, A. (1989), "Thermoacoustic refrigerations", *Cryogenic Engineering* (in Japanese), Vol. 25 No. 3, pp. 132-41.
- Yee, H.C. (1987), *Upwind and Symmetric Shock-capturing Schemes*, NASA, Washington, DC.

---

HF  
15,7

Zhu, S.W., Wu, P.Y. and Chen, Z.Q. (1990), "Double inlet pulse tube refrigerators: an important improvement", *Cryogenics*, Vol. 30, pp. 514-20.

**Further reading**

Koshimizu, T., Kubota, H., Takata, Y. and Ito, T. (2002), "Numerical simulation of heat and fluid flow in basic pulse tube refrigerator (analysis of heat exchange between wall and working gas)", *Proceeding of the 6th Symposium on Stirling Cycle*, pp. 109-12 (in Japanese).

**630**

---